Rapid and Robust Coating Method to Render Polydimethylsiloxane Surfaces Cell-Adhesive

Gehlen, David B.; Novaes, Leticia C. de Lencastre; Long, Wei; Ruff, Anna Joelle; Jakob, Felix; Haraszti, Tamas; Chandorkar, Yashoda; Yang, Liangliang; van Rijn, Patrick; Schwaneberg, Ulrich

Published in:
ACS Applied Materials & Interfaces

DOI:
10.1021/acsami.9b16025

Publication date:
2019

Biological and Medical Applications of Materials and Interfaces

Rapid and Robust Coating Method to Render Polydimethylsiloxane Surfaces Cell Adhesive

David B. Gehlen, Leticia C. De Lencastre Novaes, Wei Long, Anna Joelle Ruff, Felix Jakob, Tamás Haraszti, Yashoda Chandorkar, Liangliang Yang, Patrick van Rijn, Ulrich Schwaneberg, and Laura De Laporte

ACS Appl. Mater. Interfaces, **Just Accepted Manuscript** • DOI: 10.1021/acsami.9b16025 • Publication Date (Web): 10 Oct 2019

Rapid and Robust Coating Method to Render Polydimethylsiloxane Surfaces Cell Adhesive

David B. Gehlen,[1] Leticia C. De Lencastre Novaes,[1] Wei Long,[2] Anna Joelle Ruff,[2] Felix Jakob,[2] Tamás Haraszti,[1] Yashoda Chandorkar,[1] Liangliang Yang,[3] Patrick van Rijn,[3] Ulrich Schwaneberg,[2] and Laura De Laporte[1,4*]

[1] DWI - Leibniz Institute for Interactive Materials, Forckenbeckstraße 50, D-52074 Aachen, Germany

[2] RWTH Aachen University – Lehrstuhl fuer Biotechnologie, Worringerweg 3, D-52074 Aachen, Germany

[3] University Medical Center Groningen, Department of Biomedical Engineering-FB40, 9713 AV Groningen, The Netherlands

[4] Institute for Technical and Macromolecular Chemistry, RWTH, 52062 Aachen, Germany

E-mail: delaporte@dwi.rwth-aachen.de

Abstract: Polydimethylsiloxane (PDMS) is a synthetic material with excellent properties for biomedical applications due to its easy fabrication method, high flexibility, permeability to oxygen, transparency, and potential to produce high resolution structures in the case of lithography. However, PDMS needs to be modified to support homogeneous cell attachments and spreading. Even though many physical and chemical methods have been developed over the last decades to increase cell-surface interaction, like plasma treatment or ECM coatings, these methods are still very time consuming, often not efficient enough, complex, and can require several treatment-steps. To overcome these issues, we present a novel, robust, and fast one-step PDMS coating method using engineered anchor-peptides fused to the cell adhesive peptide-sequence (GRGDS). The anchor-peptide attaches to the PDMS surface predominantly by hydrophobic interactions by simply dipping PDMS in a solution containing the anchor-peptide, presenting the GRGDS sequence on the surface available for cell adhesion. The binding performance and kinetics of the anchor-peptide to PDMS are characterized and the coatings are optimized for efficient cell attachment of fibroblasts and endothelial cells. Additionally, the applicability is proven using PDMS based directional nanotopographic gradients, showing a lower threshold of 5 µm wrinkles for fibroblast alignment.

Keywords: Polydimethylsiloxane, protein engineering, anchor peptide, liquid chromatography peak I, LCI, RGD, bioactive surface coating, cell adhesion.

New, highly biocompatible devices are under constant development to better integrate with native organs and tissues in a controllable manner. One of the common materials used for these devices is polydimethylsiloxane (PDMS) as it has outstanding properties like low cost, easy fabrication procedure, permeability to oxygen, optical transparency in visible and ultraviolet light, and its flexible nature.[1] These features render PDMS to be an ideal material for many biomedical applications, such as heart valves,[2] extracorporeal lung devices with improved transport properties,[3-5] microfluidic devices[6] for lab-on-a-chip[7-8] and organ-on-a-chip[9-10] applications, or as a substrate to study (stem) cell behavior. The latter is of great interest to better understand the effects of stiffness,[11] topography,[12-13] stretching,[14] and electrical[15] or mechanical stimulation[16] on cells, which is crucial information for designing biomaterials with the purpose of tissue engineering and regenerative medicine, or to improve biointegration of medical devices. One remaining limitation to use PDMS for biomedical devices is the challenge to achieve a high interaction with cells. Therefore, many approaches are developed to either physically change the surface properties or to physically or chemically bind molecules to the surface. Large bioactive extracellular matrix (ECM) proteins are often used to render surfaces cell adhesive, while specific short amino acid sequences from several large ECM proteins can selectively modify substrates, depending on the cell type and its integrins.[17] In the case of expensive ECM proteins, batch to batch variations and potential pathogens depending on the source can cause additional problems.

One easy way to chemically change the surface properties of a substrate is an oxygen plasma treatment to generate hydroxy-groups on the surface.[18] However, this method does not allow to alter the surface properties of PDMS in a controlled manner and is not stable due to hydrophobic recovery, which occurs due to reorientation and condensation of the hydroxy-groups. Similar modification to this are microwave plasma,[19] deep UV and ozone treatment,[20] and KOH treatment,[21] which face the same limitations as the previous method. In order to control the (biochemical) properties of the surface, coatings with ECM proteins, like fibronectin, are applied onto PDMS surfaces pre-treated with, for example, sodium hydroxide.[22] This method requires a multi-step treatment and the protein adsorption is unspecific, often leading to a non-homogeneous coating and the risk that the functionality of the proteins may partially be impaired. To covalently attach ECM proteins to the surface in a stable manner, (3-aminopropyl)triethoxy

silane (APTES) and glutaraldehyde (GA)[23] are used as a crosslinker, while N-sulfosuccinimidyl-6-(4'-azido-2'-nitrophenylamino) hexanoate (sulfo-SANPAH) has been employed as a bifunctional photolinker to attach short adhesive peptides.[24] However, the used compounds are toxic and lead to toxic wastes, a multi-step treatment is necessary, and it cannot be excluded that the reaction affects the bioactive domains of the proteins. To overcome the challenges with toxicity, a recent method uses polydopamine as a coating agent.[25] Due to oxidative polymerization at pH 8.5, catechol oxidizes to quinone, resulting in covalent bonds and strong intermolecular interactions via hydrogen-bonds, metal chelation, and π-π interactions with PDMS.[26-28] Polydopamine can interact with the amines of endogenous ECM proteins produced by the cells,[29] or be used as a linker for added ECM proteins, representing a multi-step process again. In both cases, the binding may interfere with protein activity.

In order to achieve an environment-friendly, robust, and fast one-step coating without uncontrolled crosslinking reactions between a coating agent and the bioactive compound, the cell adhesive peptide sequence (GRGDS) is fused to the anchor peptide LCI (liquid chromatography peak I) and the fusion peptide is produced with *Corynebacterium glutamicum*. The anchor peptide LCI originates from *Bacillus subtilis* and belongs to the class of antimicrobial peptides, which typically contain between 10 and 100 amino acids, interact with lipid membranes, are water soluble, and are stable at room temperature.[30-32] The utilization of antimicrobial peptides as adhesion promoters for polymeric materials was previously reported: Cecropin A was used for the decoration of polymersomes,[33] while polypropylene was functionalized with a monomolecular layer of LCI-eGFP, as proven by scanning force microscopy (SFM).[30-31] The binding strength of LCI to polypropylene and polystyrene was improved by the presence of surfactants in direct evolution campaigns.[31, 33-35] As the anchor peptide LCI binds to the aforementioned hydrophobic polymers, it is here selected to test its coating efficiency of highly hydrophobic PDMS surfaces. The interaction with the hydrophobic surface is not completely understood. In previous reports, Horinek and collaborators have shown that the adsorption of a mildly hydrophobic peptide from water to a solid hydrophobic surface is governed by a complex interplay of opposing interactions that largely compensate each other. They state that the hydrophobic attraction between the peptide and the surface cannot be solely explained by one single mechanism.[36] The

LCI structure is composed of hydrophobic and hydrophilic residues, which provide a well balance of hydrophobic and hydrophilic interactions with surfaces. The interaction of LCI with polymers like polypropylene, polystyrene, and polyethylene terephthalate was described in our previous study, were contact angle measurements indicated that the hydrophilic residues are likely to be exposed to the aqueous phase.[37-38] It is important to point out that the LCI anchor peptide contains four tyrosines and is rich in hydrophobic amino acids, such as isoleucine, valine, and phenylalanine. This leads to a peptide structure with hydrophobic and hydrophilic regions, allowing the peptide to interact with the surface via the hydrophobic regions, while the hydrophilic regions are important for solubility in water. Thus, for the LCI anchor peptide, a complex interplay of interactions takes place, among which the side chains of isoleucine, valine, and phenylalanine can interactions with hydrophobic surfaces (e.g. via hydrophobic interactions with CH_3 groups).

To analyze the binding properties and kinetics of the anchor peptide LCI, the enhanced green fluorescein protein (eGFP) is fused to the anchor peptide (eGFP-LCI), allowing to measure the fluorescence intensity of the treated surfaces. In a first step, a constant concentration of eGFP-LCI (125 nM) is incubated on PDMS surfaces for different times at room temperature (**Fig. 1 A**). After washing of the samples, the fluorescence is detected with a Biotech® plate-reader. The measured data points are fitted according to a pseudo-first-order kinetic ($y = A (1 - e^{-k \cdot t})$) revealing a very fast binding within the first ten minutes and a much slower gradual binding after ten minutes. After optimizing the incubation time, different concentrations, ranging from 15.6 nM to 1.0 µM, are applied to PDMS surfaces for a constant time of 10 minutes to evaluate that the coating density can be varied (**Fig. 1 B**).

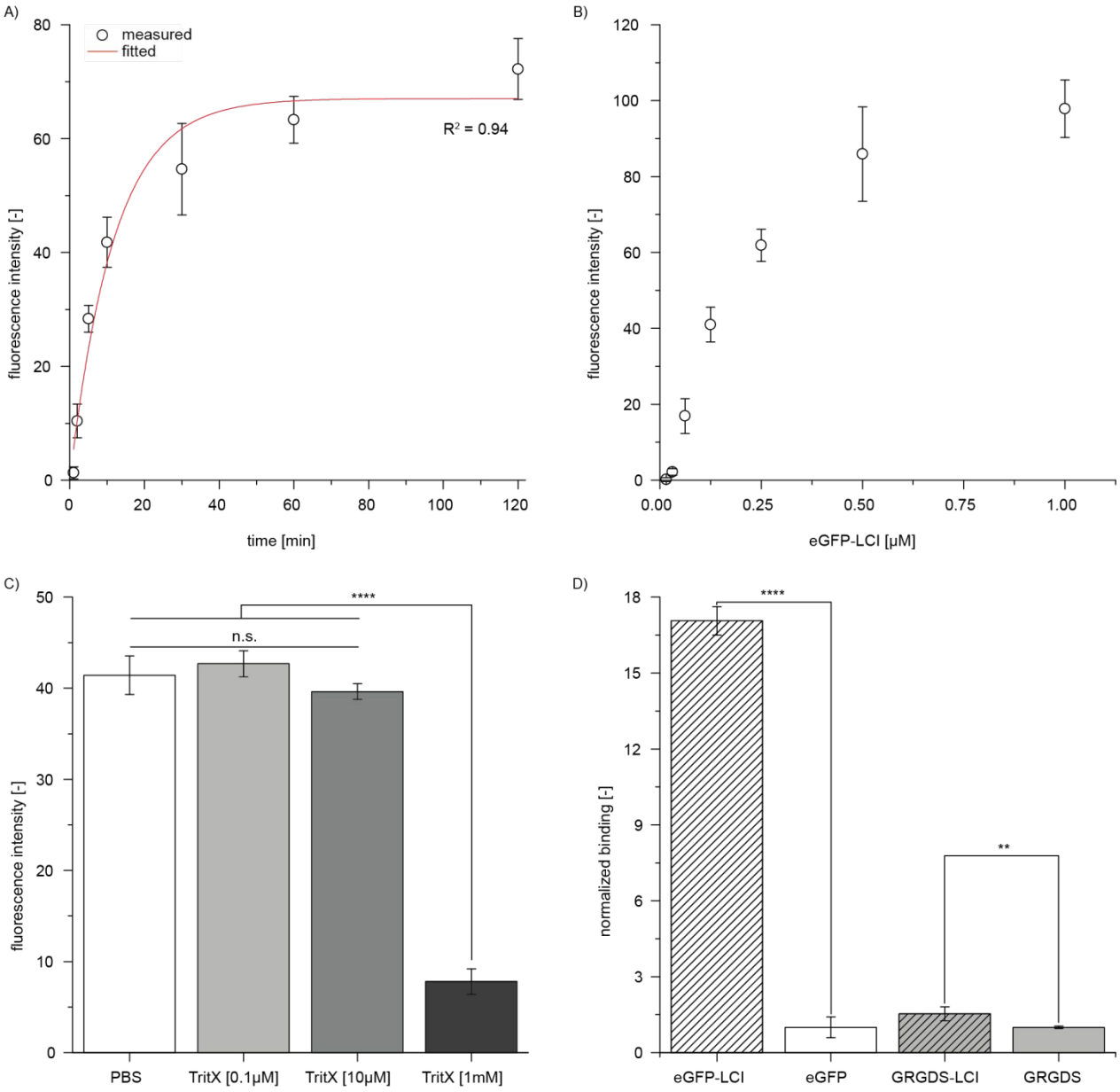

Fig. 1: A) Different incubation times of 125 nM (0.125 µM) eGFP-LCI and fitting of the data reveal that most of the anchor peptides bind to the PDMS surface within the first 10 min. B) Different concentrations of the anchor peptide in solution results in different fluorescence intensities on the surface (coating density) up to 1.0 µM. C) Stability of eGFP-LCI coatings on PDMS towards Triton X-100 in PBS (1x, pH 7.4) with different concentrations (0.1 µM, 10 µM, 1.0 mM) compared to only treated with PBS (1x, pH 7.4). D) Normalized binding of eGFP and immunostained RGD with and without fused anchor peptide reveal a 1.5-17 fold increase in binding of the compounds with the fused anchor peptide LCI.

In previous studies, we showed high stability towards surfactants on polypropylene surfaces.[30] The high stability towards surfactants is also of great importance for the anchor peptide on PDMS

for cell culture applications since serum-containing solutions contain proteins that function as efficient surfactants. Therefore, to prove the stability of the anchor peptide on PDMS towards surfactants, coated PDMS-surfaces are treated with Triton X-100 solutions in PBS (1x, pH 7.4) at different concentrations at room temperatures for 15 minutes, revealing a high stability towards surfactants even at high concentrations up to 10 µM Triton X-100 comparable to surfaces treated only with PBS (1x, pH 7.4) (**Fig. 1 C**). Furthermore, the long term stability of the eGFP-LCI coating is analyzed up to two weeks, showing that the fluorescence intensity and, thereby, the coating is still stable and has not changed after 14 days (**Fig. S1**).

The binding of eGFP-LCI is compared with the binding of eGFP without an anchor peptide, revealing a significant 17-fold increase in normalized fluorescence signal (f[eGFP-LCI]/f[eGFP]). Additionally, the anchor peptide LCI linked to the cell adhesive GRGDS peptide-sequence is used for surface coating (1.0 µM), as well as GRGDS alone. Both are subsequently immunostained with anti-GRGDS, demonstrating a 1.5 fold higher binding forGRGDS-LCI, compared to GRGDS (**Fig.1 D**).

After optimizing the coating conditions, different concentrations of GRGDS-LCI (250 nM - 8 µM) are applied to PDMS surfaces to study the effect on mouse fibroblasts (L929). PDMS surfaces treated with a high concentration of GRGDS (100 µM) are used as a negative control and normal tissue culture polystyrene (TCPS) as a positive control. After two days of incubation, efficient cell attachment and spreading, comparable to TCPS surfaces, is observed for GRGDS-LCI concentrations above 1.0 µM, whereas round and non-adhering cells are present on the negative control (GRGDS without the anchor peptide). Below 1.0 µM of GRGDS-LCI, the cells only partially spread and adhere, indicating that 1.0 µM is the threshold for achieving satisfactory cell attachment (**Fig.2 A**). After two days of incubation, a proliferation assay is performed. The absorbance at λ = 490 nm, which corresponds to the cell's metabolic activity, shows no difference between the positive control (TCPS) and PDMS coated with GRGDS-LCI above concentrations of 1.0 µM. The values are slightly lower but not significant for concentrations below 1.0 µM, which is in accordance with the appearance of the cells. In contrast, using PDMS treated with GRGDS without an anchor peptide or untreated PDMS (only water) results in significantly lower metabolic activities and much lower cell attachment (**Fig. 2 B**). Based on these results, 1.0 µM of GRGDS-LCI

is considered to be an optimal concentration for PDMS coating to achieve satisfactory mouse fibroblast cell attachment.

For better visualization of the fibroblasts adhered to the coated PDMS surface, the F-actin filaments are stained with Phalloidin-iFluor 488 CytoPainter (green), illustrating a highly spread morphology of the cells (**Fig. 2 C**). Additionally, a Live/Dead assay is performed where green (alive) spreading cells are observed on the GRGDS-LCI coated PDMS, while round and many red (dead) cells are present on the control surfaces, confirming the successful bioactivation of the PDMS surface with GRGDS-LCI (**Fig. 2 D**).

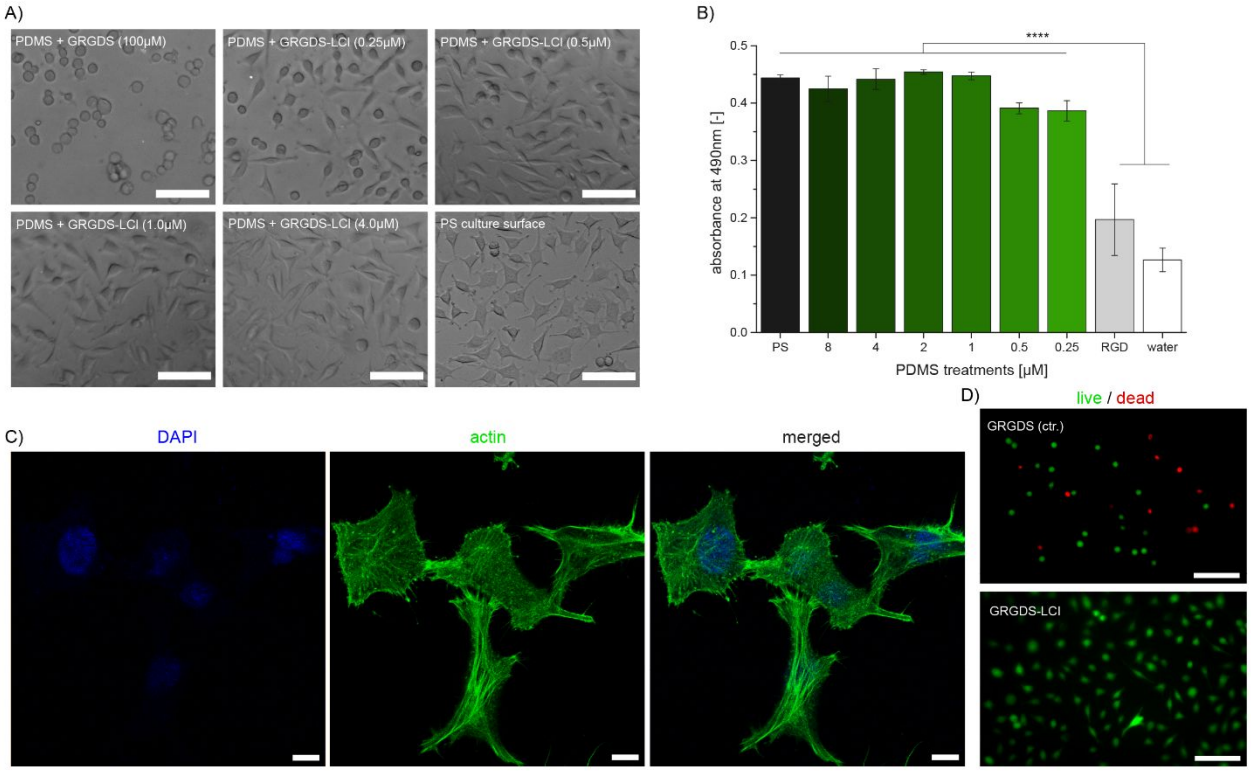

Fig. 2: A) Bright field images of fibroblasts on GRGDS treated and subsequently washed PDMS surfaces showing no adhesion, whereas the cells adhere partially to PDMS treated with 0.25 and 0.5 µM of GRGDS-LCI and completely on PDMS treated with 1.0 µM and higher concentrations of GRGDS-LCI, comparable to the normal TCPS culture surface. B) MTS assay showing comparable proliferation of cells on GRGDS-LCI treated PDMS with TCPS surfaces, whereas proliferation is significantly reduced on GRGDS treated (100µM) and untreated (water) PDMS (N=3). C) DAPI (blue) and-F-actin (green) staining of fibroblasts on 1.0 µM GRGDS-LCI functionalized PDMS showing highly spreading cells on the surface. D) Live/dead staining of fibroblasts on GRGDS-LCI (1.0 µM) coated PDMS reveals vital and adhesive cells, whereas non-adhesive and dead cells are observed in the controls. Scale bars represent 10 µm for C) and 100 µm for D).

To prove applicability for other cell lines, human umbilical vein endothelial cells (HUVECs) are cultivated on PDMS coated with different GRGDS-LCI concentrations between 125 nM and 4.0 µM, using the same controls as mentioned above. HUVECs present similar results as for mouse fibroblasts. On PDMS coated with GRGDS-LCI above concentrations of 1.0 µM, the cells attach to the surface and the morphology is spread, comparable to the TCPS positive control. Below 1.0 µM of GRGDS-LCI, the cells round up and form clusters, demonstrating that they cannot attach to the surface in a satisfactory manner. In the case of the PDMS treated with GRGDS without the anchor peptide, the cells show even less cell attachment (**Fig. 3 A**). Quantification using a proliferation assay confirms this observation, showing high metabolic activity for cells cultivated on GRGDS-LCI treated surfaces above concentrations of 1.0 µM, comparable to the TCPS control while decreasing at concentrations below 1.0 µM. For untreated PDMS and GRGDS, no metabolic activity is detected in contrast to the fibroblasts, indicating that no HUVECs are able to attach to the surface and are washed away during the proliferation assay (**Fig. 3 B**). Based on these results, 1.0 µM of GRGDS-LCl is again considered as an optimal concentration for PDMS coating to achieve satisfactory adhesion of HUVECs.

For visualization of cell morphology, the F-actin skeleton of the cells is stained using Phalloidin-iFluor 488 CytoPainter (green), while the adhesion molecule VE-cadherin is stained (red) to display the cell junctions between the endothelial cells. On the GRGDS-LCI functionalized PDMS surface, cells are well spread, indicating a high cell attachment. The strong VE-cadherin signal at the edge of the HUVECs demonstrates that cells interact strongly with their neighboring cells (**Fig. 3 C**). Cells further away from their neighbors show most of the VE-cadherin signal in the middle of the cells and not at the edge. To achieve a confluent cell layer, which is often desired for biomedical applications, cells have to adhere, spread, and proliferate to build up a high density cell layer with strong cell-matrix and cell-cell interactions. For analyzing the cell viability of HUVECs on GRGDS-LCI treated PDMS surfaces, a Live/Dead assay is again performed, revealing vital (green) and spread cells, whereas the control shows only a few and round cells as most cells are washed off during the analysis (**Fig. 3 D**).

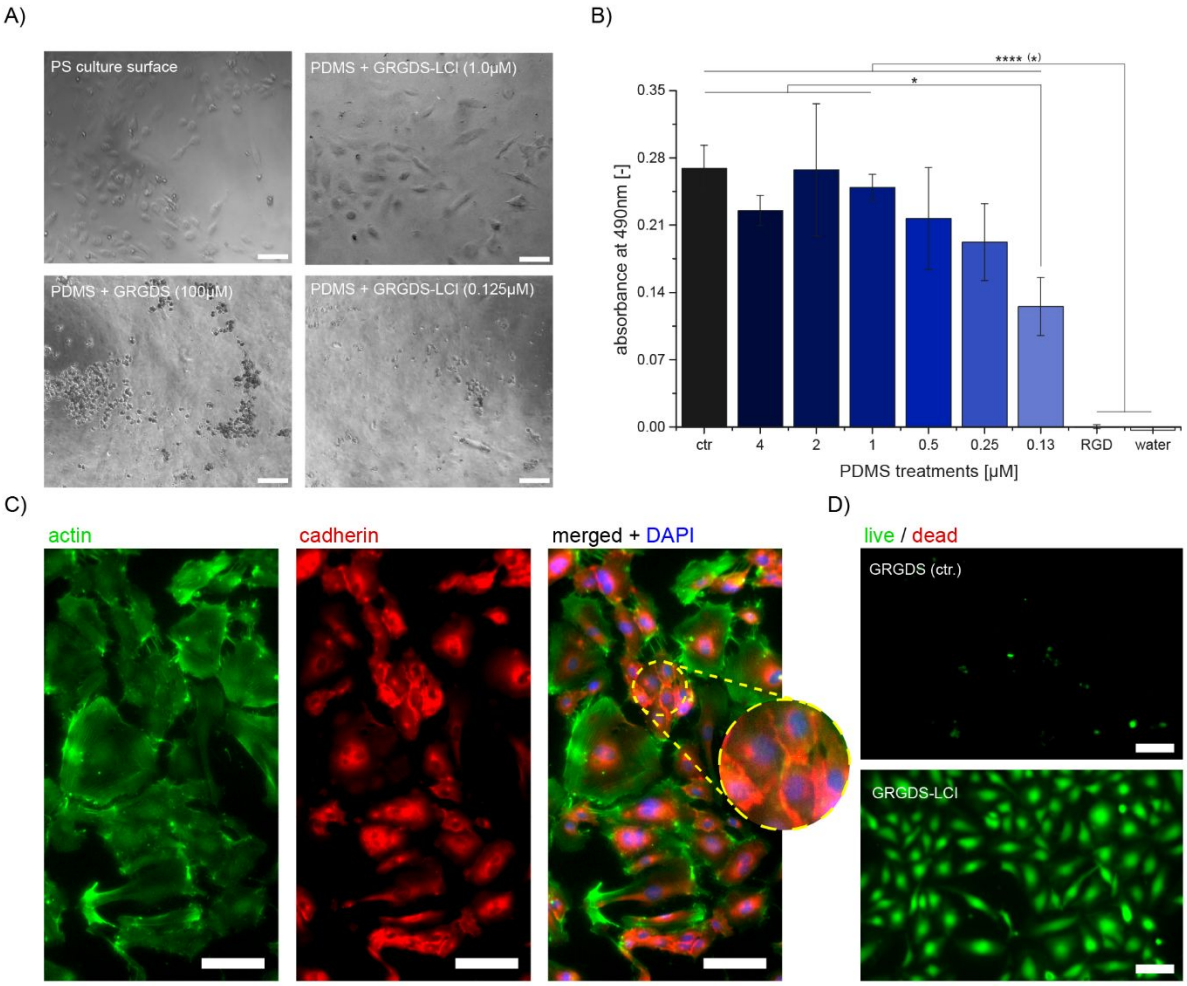

Fig. 3: A) Bright field images of HUVECs on GRGDS treated and subsequently washed PDMS surfaces showing a round non-adhesive morphology, whereas the cells are only partially round on PDMS treated with 0.125 µM of GRGDS-LCI and completely flat and adhesive on PDMS treated with 1.0 µM of GRGDS-LCI, comparable to a normal PS culture surface. B) MTS assay showing comparable proliferation of cells on GRGDS-LCI treated PDMS (≥ 1 µM) comparable to PS culture surface, whereas no proliferation is detected on GRGDS treated (100 µM) and untreated (water) PDMS, (RGD and water significant different with * to 0.13 µM GRGDS-LCI and **** to all other conditions; N=3). C) Immunostaining of F-actin and VE-cadherin, respectively, shows a spread cell morphology and cell-cell interaction in areas where the cell density is high enough. D) Live/Dead assay reveals no cells in the control (GRGDS), whereas many spread and vital cells are observed for the GRGDS-LCI treated surface. Scale bars represent 100 µm.

As an application example for the newly developed coating method for biomedical devices, PDMS based directional nanotopographic gradients (**Fig. S2**)[39-40] are dip-coated with the GRGDS-LCI and seeded with fibroblasts (**Fig. 4 A**). The PDMS surfaces contain parallel wrinkles with sizes ranging

from 1 to 14 µm. After three days of incubation, the cells are fixed and the F-actin skeleton is stained using Phalloidin-iFluor 488 CytoPainter to analyze cell alignment. On PDMS without guiding elements, the cells grow randomly in all directions, whereas on small 3 µm wrinkles, they start to grow partially in the direction of the elements. On 9 µm wrinkles, the cells are highly aligned and spread along with the wrinkles (**Fig. 4 B**). The cell alignment based on cell morphology is quantified as previously described using the F-actin channel (**Fig. 4 C**).[41] For a flat PDMS surface, the signal shows almost the same intensity in all direction (-90° to +90°), demonstrating that the cells do not have a preferred direction. On the other hand, surfaces with 3 µm wrinkles show most of the signal in one direction, indicating a preferred direction, while in the case of 9 µm wrinkles, almost all of the signal is focussed in one direction, proving high cell alignment (**Fig. 4 D**). Based on the signal distributions, the full width half maximum (FWHM) is determined. A lower FWHM indicates a narrow distribution and correlates with more aligned cells. At least ten images per condition are used to determine the FWHM for different wrinkle sizes and for flat PDMS as a control. The quantification confirms the observation that slightly aligned cells are present on wrinkles ≤ 3 µm, while better alignment is seen for larger ridges (**Fig. 4 E**). For wrinkles above 5 µm, all cells show the same FWHM, illustrating that 5 µm is an important threshold for fibroblasts alignment on contact guiding elements.

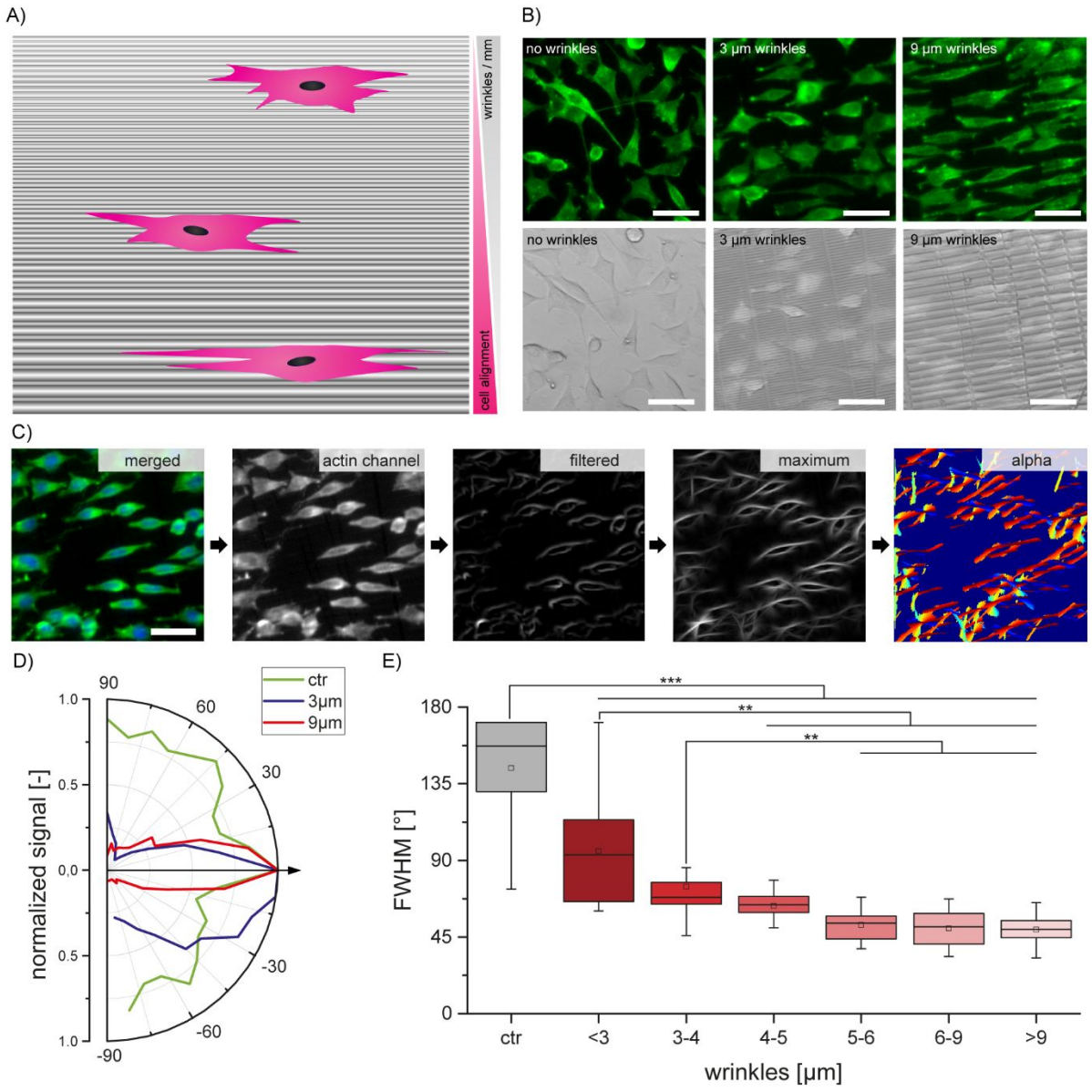

Fig. 4: A) Cartoon of a PDMS based directional nanotopographic gradient showing the effect on cell alignment based on the size of the wrinkles. B) F-actin skeleton of fibroblasts (green) and topography of the PDMS (grey) for flat PDMS, 3 µm wrinkles, and 9 µm wrinkles showing random growth for flat PDMS and high alignment on 9 µm wrinkles. C) Quantification of alignment: 200x200 µm regions of interest of the F-actin-channel, which are sequentially filtered, and calculated into a maximum orientation-intensity image, leading to an alpha image for the quantification of cell alignment. D) Distribution of the signal showing no predominant direction for the flat PDMS control, a predominant direction for 3 µm wrinkles, and high cell alignment/narrow distribution for 9 µm. E) A full width half maximum (FWHM) analysis reveals random growth for PDMS without a topography, an increase in alignment until 5 µm wrinkles, above which the maximal alignment does not further increase. Scale bars represent 50 µm.

In summary, the here presented functionalization method for PDMS surfaces, based on anchor peptides, allows for an easy and fast coating of PDMS compared to previously developed methods. Only one incubation step with GRGDS-LCI, as short as 10 min, is required to achieve a high density of bioactive peptides on a PDMS substrate in a controlled manner without the need for chemical linking reactions. Two cell lines, fibroblasts and endothelial cells, are tested and reveal spreading and proliferation of viable cells for a concentration of 1 µM GRGDS-LCI. Biomedical devices can simply be dipped in the anchor peptide solution, allowing to rapidly and effectively coat complex structures, which is often a limiting factor for other commonly used methods, like sulfo-SANPAH. Since the coating takes place under mild conditions at room temperature, complex biomedical devices containing sensitive parts can be easily functionalized.

Additionally, the bioactivity can be tailored by linking other functional peptides or proteins to the anchor peptide. Translating this technology to other fused cell-adhesive peptides for specific applications would involve constructing, expressing, and purifying these peptides, which requires specific equipment in the lab. In order to achieve broader applicability, the LCI anchor peptide could potentially be functionalized with N-Hydroxysuccinimid (NHS), allowing secondary coupling of a variety of existing peptides and bioactive molecules. Even though this has the drawback of being a two-step process, it would facilitate more flexible use of the peptide for a wider range of applications. On the other hand, as GRGDS is still the most commonly used cell adhesive peptide, commercialization of the GRGDS-LCI would also enable its wide-spread use. The method can modify PDMS surfaces in a controllable manner for maximal attachment of different types of cells in for example “lab on a chip” or “organs on a chip” applications for drug screenings or stem cell behavior studies, or for coating of artificial heart valves or comparable medical devices. In the future, engineering the backbone of the anchor peptide may enable the development of smart coatings, which are for example pH-sensitive or have specific affinities to hydrophilic or hydrophobic patterns on a substrate.

Materials and Methods:

Materials: All used chemicals are purchased from Sigma-Aldrich Corp. (St. Louis, MO, USA), AppliChem GmbH (Darmstadt, Germany), as well as Carl Roth GmbH (Karlsruhe, Germany) and had analytical-reagent grade or higher purity. Oligonucleotides are acquired from Eurofins Scientific SE (Ebersberg, Germany) in salt-free form. Enzymes are obtained from New England Biolabs GmbH (Frankfurt am Main Germany). Plasmid extraction and PCR purification kits are purchased from Macherey-Nagel GmbH & Co. KG (Düren, Germany) and Qiagen GmbH (Hilden, Germany). The BCA Protein Assay kit is obtained from Novagen EMD Chemicals Inc. (San Diego, USA).

Plasmids and strains Plasmid: Plasmid pET28a(+) from Novagen (Darmstadt, Germany) and the plasmid pEKEx2 (received from Prof. Dr. Roland Freudl, IBG-1: Biotechnology, Institute of Bio- and Geosciences, Forschungszentrum Jülich GmbH, Germany) (GenBank: AY585307.1) are used as expression vectors. *Escherichia coli* strains DH5α and BL21-Gold (DE3) are purchased from Agilent Technologies (Santa Clara, CA) and the *Corynebacterium glutamicum* ATCC 13032 is received from Prof. Dr. Roland Freudl (IBG-1: Biotechnology, Institute of Bio- and Geosciences, Forschungszentrum Jülich GmbH, Germany). *E. coli* DH5α is used as cloning host, *E. coli* BL21-Gold (DE3) and *C. glutamicum* are used for protein expression.

The amino acid sequence of LCI (PDB ID: 2B9K) is: [35]

AIKLVQSPNGNFAASFVLDGTKWIFKSKYYDSSKGYWVGIYEVWDRK

Methods:

Generation, production and purification of EGFP-LCI fusion construct: Fusion protein of anchor peptide LCI with eGFP is generated to simplify detection and quantification of bound LCI on PDMS surface. The fusion protein consists of an N-terminal eGFP, which was functionally separated by a stiff spacer helix (17 amino acids: AEAAAKEAAAKEAAAKA)[42] and a TEV cleavage site (7 amino acids: ENLYFQG)[43] from the C-terminal LCI. The construct pET28a::eGFP-17xHelix-TEV-LCI is generated as previously described[30]. The generated fusion protein eGFP-LCI and the negative

control eGFP (without LCI) are expressed in *E. coli* BL21 (DE3) gold cells with subsequent chromatography purification and dialysis as previously described[30]. Protein concentrations are determined with the BCA protein assay kit (Novagen, Merck KGaA) and protein homogeneity is analyzed by sodium dodecyl sulfate polyacrylamide gel electrophoresis (SDS- PAGE) using a 5% stacking and a 12% separating gel[44].

Generation, production and purification of GRGDS-LCI fusion construct: The 17xHelix-TEV-LCI is cloned in the pEKEx2::Npre backbone applying "sequence independent phosphorothioate-based ligase-independent gene cloning" (PLICing)[45]. Target sequence (17xHelix-TEV-LCI) is amplified using primers F-Insert and R-Insert containing phosphorothioated nucleotides. The vector backbone pEKEx2::Npre is amplified using primers F-Vector and R-Vector. The parental DNA is digested (20 U DpnI, 16 hr, 37°C) and purified (QIAquick PCR Purification Kit, QIAGEN, Hilden, Germany). Iodine cleavage and hybridization is performed with 0.2 µM insert and 0.004 µM vector. The generated construct is used for transformation of *E. coli* DH5a cells. Successful construction of the plasmid is verified by sequencing (Eurofins Genomics GmbH, Ebersberg, Germany). The insertion of the GRGDS sequence is performed by overlap extension PCR[46]. The amino acid sequence GRGDS is fused to the N-terminus of the 17xHelix resulting in the genetic construct pEKEx2::Npre-GRGDS-17xHelix-TEV-LCI. The PCR product is digested (20 U DpnI; overnight, 37 °C) and purified using PCR clean-up kit (Macherey-Nagel), transformed and the insertion of the correct sequence is subsequently verified by sequencing. The fusion protein GRGDS-LCI (plasmid: pEKEx2::Npre-GRGDS-17xHelix-TEV-LCI) is expressed in *C. glutamicum*. A single colony is transferred to 5 mL of BHIS medium (37 g/L brain heart infusion, 91 g/L sorbitol, 0.1 mM kanamycin) and incubated overnight (16 h, 30°C, 200 rpm, Multitron Pro, Infors AG, Bottmingen, Switzerland). The pre-culture is used to inoculate the main culture (100 mL BHIS) to an OD_{600nm} of 0.05. The main culture is cultivated until the OD_{600nm} of 0.6 is reached (4 h, 30°C, 200 rpm). Protein over-expression is induced by supplementing isopropyl b-D-1-thiogalactopyranoside (IPTG; 0.1 mM final concentration). Upon induction, the cultivation temperature is reduced to 25°C. Cells are harvested after 48 h by centrifugation (3200 g, 20 min, 4°C; Eppendorf centrifuge 5810 R, Eppendorf AG, Hamburg, Germany). The supernatant is filtered through a 0.45 mm cellulose-acetate filter (GE Healthcare, Little Chalfont, UK) and subsequently

used for protein purification. The GRGDS-LCI fusion protein contains a Strep-Tag and is purified using a fast protein liquid chromatography system (ÄKTAprime, GE Healthcare) with a prepacked Strep-Tactin affinity chromatography column (Strep-Tactin Superflow Plus Cartridges, 5 mL, Quiagen). Samples are desalted using a dialysis membrane (Spectra/Por®4, Spectrum Inc., Breda, The Netherlands) and concentrated using ultra centrifugal filters (Amicon Ultra-15 15mL - 3 KDa cutoff, Merck KGaA, Darmstadt, Germany) for further cell growth studies.

Preparation of PDMS surfaces: For preparing PDMS surfaces, 10.0 g of Sylgard® 184 (Dow Corning) and 1.0 g of the initiator (Dowsil) are rigorous mixed and air bubbles are removed via centrifugation at 1,500 rpm for 5 min. For PDMS coated wellplates, 100 µL of the solution is filled in 96 wellplates (Greiner Bio-One) and cured at 40 °C overnight. For PDMS discs, PDMS is poured in Petri dishes to obtain a 1 mm thick film, which is cured at 40 °C overnight. Discs with the size of either 96 or 48 wellplates are punched out of the PDMS film. The production of the PDMS based directional nanotopographic gradients is described elsewhere.[39-40]

Analyzing binding parameters of LCI: Fused eGFP-LCI is used for analyzing the binding kinetics in order to measure the fluorescence intensity of the eGFP on the coated surfaces. The anchor peptide is diluted in phosphate buffered saline (PBS, Lonza) with a concentration of 125 nM and 110 µL of the final solution is added to PDMS coated 96 wellplates. The solution is incubated at room temperature under the exclusion of light for different times between 1 and 120 min and subsequently washed three times with 200 µL of PBS on a shaker for two minutes. For quantification of the fluorescence intensity, 100 µL of PBS are added to the wells and the fluorescence is measured with an excitation wavelength of 485/20 nm and an emission wavelength 528/20 nm using a Biotech® plate-reader. The coating concentration is analyzed in the same way using a fixed incubation time of 10 min and concentrations between 15.6 nM and 1.0 µM. For visualization of the binding, eGFP-LCI and GRGDS-LCI, or eGFP and GRGDS without an anchor peptide at the same concentrations, are used for functionalization. GRGDS-LCI and GRGDS are immunostained with an anti-GRGDS antibody (Biorbyt). After washing, the binding is quantified by measuring the fluorescence using a Biotech® plate-reader with an excitation wavelength of 485/20 nm and an emission wavelength 528/20 nm. For normalization, the fluorescence signal of the sample (eGFP-LCI and GRGDS-LCI) is divided by the fluorescence signal

of the control (eGFP and GRGDS without an anchor peptide). To analyze the stability towards surfactants, different concentrations of Triton™ X-100 solutions (0.1 µM, 10 µM, and 1.0 mM) in PBS (1x, pH 7.4) are incubated on eGFP-LCI coated PDMS surfaces for 15 min at room temperature. The PDMS surfaces were coated with 125 nM of eGFP-LCI for 10 minutes. Treatment with PBS (1x, pH 7.4) instead of a Triton™ X-100 solution is used as a control. Subsequently, the surfaces are washed three times with PBS (1x, pH 7.4) and the remaining fluorescence signal is measured. In order to measure the long term stability of the anchor peptide coatings on PDMS, eGFP-LCI coated PDMS surfaces (125 nM of eGFP-LCI) are stored in PBS (1x, pH 7.4) at room temperature and the fluorescence intensity is measured on day 0, 7, and 14.

Cell experiments: In a first step, the PDMS surfaces are disinfected using 70 vol% of ethanol for 30 min and 30 min of UV radiation. The sterilized samples are washed three times with 1x PBS, followed by applying the anchor peptide at different concentrations and incubation at room temperature for 10 min. For the negative controls, either only water or a high concentration of RGD without anchor peptide (100 µM) are added and incubated at room temperature for 10 min. Subsequently, the surfaces are washed three times with PBS on a shaker, after which cells are seeded on the surface. Mouse derived fibroblasts (L929, Lonza) are cultivated in RPMI media 1640 (Lonza) supplemented with 10 vol% of fetal bovine serum (FBS, Biowest) and 1 vol% Gibco™ antibiotic-antimycotic at 37 °C and 5 vol% CO_2 with a seeding density of 5,000 N/well for 96 wellplates, and 20,000 N/well for 48 wellplates. An incubation time of two days is chosen to ensure enough time for cell attachment and a longer incubation time of three days to obtain sufficient cell density on the PDMS based topographic gradients. Endothelial cells (HUVECs, Lonza) are cultivated using Clonetics™ EGM™-2MV BulletKit™ (Endothelial Basal Medium-2 (EBM™-2 medium) with growth supplements, Lonza) with a density of 10,000 N/well in 96 wellplates and are cultivated for three days to enable cell-cell interactions. To perform a proliferation assay, the media is removed and replaced by 150 µL of a (3-(4,5-dimethylthiazol-2-yl)-5-(3-carboxymethoxyphenyl)-2-(4-sulfophenyl)-2H-tetrazolium) (MTS, Promega) solution in media, which is incubated for 2-4 h on the cells. An incubated MTS solution without cells is used as a blank. After incubation, 100 µL per sample is transferred to a new 96 wellplate and the absorbance is measured at a wavelength of 490 nm using a Biotech® plate-reader. For the

optimized coating concentrations (1.0 µM GRGDS-LCI) and for the control (GRGDS), a live/dead assay is performed using a Live/Dead® Viability/Cytotoxicity kit for mammalian cells (Biovision). Here, 1.0 µL of the Live Cell Staining Dye and 0.5 µL of the Dead Cell Staining Dye are diluted in 500 µL assay buffer and used to replace the media on the cells. After 30 minutes of incubation, the samples are analyzed using fluorescence microscopy. The wavelength for live cells is 530 nm and 645 nm for dead cells.

Immunostaining: After cultivation, the cells are washed once with PBS (1x, pH 7.4), fixed for 30 min in 4 w% of paraformaldehyde (PFA, AppliChem) and washed again three times with PBS (1x, pH 7.4). The samples are then blocked with 4 w% bovine serum albumin (BSA, Sigma-Aldrich) in PBS (1x, pH 7.4) for 30 min and stained with the first antibody: polyclonal anti-VE Cadherin antibody produced in rabbit 1:500 (abcam) and Phalloidin-iFluor 488 CytoPainter (abcam) in 4 w% BSA in PBS (1x, pH 7.4) at room temperature overnight. The samples are washed three times with PBS (1x, pH 7.4) and stained with the secondary antibody: goat anti-rabbit IgG (H+L) Alexa Fluor 568 1:100 (Thermo Fisher Scientific). Next, the samples are stained with 3 µM of 4',6-Diamidin-2-phenylindol (DAPI, Thermo Fisher Scientific) in PBS (1x, pH 7.4) for 30 min and washed three times with PBS (1x, pH 7.4). For anti-GRGDS immunostaining, the surfaces are incubated with polyclonal anti-GRGDS antibody, produced in rabbit, 1:100 in PBS (1x, pH 7.4) (Biorbyt) at room temperature overnight and washed three times with PBS (1x, pH 7.4). Next, goat anti-rabbit IgG (H+L) Alexa Fluor 488 (Thermo Fisher Scientific) 1:100 in PBS (1x, pH 7.4) is incubated for 2 h at room temperature and subsequently washed three times with PBS (1x, pH 7.4). Fluorescence microscopy is performed using a Leica DMIL LED Fluorescence microscope, Leica SPi8, or with a Zeiss Axio Observer Z1 microscope equipped with an AxioCam MRm camera. Image processing is performed using LasX, AxioVision and ImageJ.

Quantification: For analyzing cell alignment on PDMS based directional nanotopographic gradients, the actin channel is chosen and 200x200 µm regions of interest (ROI) are selected and cut out to ensure comparable amounts of cells per analyzed field. Next, the sizes of the wrinkles within the ROI are determined using the brightfield channel and the ImageJ measuring tool. The ROI of the actin channel is subsequently background corrected and processed with an edge detector filter. Anisotropic, Gaussian orientation kernels (with 20 directions between -90 and +90

degrees) were convolved with the filtered image, and calculated into a maximum intensity image, leading to an alpha image of best matched orientation at each pixel, for quantification of the cell alignment, as previously described.[41] Next, the distribution of the angles for different wrinkle sizes is determined and compared using their FWHM.

Statistics: Statistics are analyzed using OriginPro 2016G. A one-way ANOVA is performed with a Tukey comparison to determine statistical significance. Data points are shown as mean average with error bars indicating the standard deviation and the p values for statistical significance is represented with stars: *$p < 0.05$, **$p < 0.01$, ***$p < 0.001$, ****$p < 0.0001$.

Acknowledgments:

The authors acknowledge the European Commission (EUSMI, 731019) and Frederik Stolz for solving general laboratory workflow issues. This work was performed in part at the Center for Chemical Polymer Technology CPT, which was supported by the EU and the federal state of North Rhine-Westphalia (grant EFRE 300088302).

Associated content:

Supporting information is provided (Figure S1-2).

References:

(1) Mata, A.; Fleischman, A. J.; Roy, S. Characterization of Polydimethylsiloxane (PDMS) Properties for Biomedical Micro/Nanosystems. *Biomedical Microdevices* **2005,** *7* (4), 281-293.
(2) Rippel, R. A.; Ghanbari, H.; Seifalian, A. M. Tissue-Engineered Heart Valve: Future of Cardiac Surgery. *World Journal of Surgery* **2012,** *36* (7), 1581-1591.
(3) Hoganson, D. M.; Pryor II, H. I.; Bassett, E. K.; Spool, I. D.; Vacanti, J. P. Lung Assist Device Technology with Physiologic Blood Flow Developed on a Tissue Engineered Scaffold Platform. *Lab on a Chip* **2011,** *11* (4), 700-707.
(4) Femmer, T.; Eggersdorfer, M. L.; Kuehne, A. J.; Wessling, M. Efficient Gas–Liquid Contact Using Microfluidic Membrane Devices with Staggered Herringbone Mixers. *Lab on a Chip* **2015,** *15* (15), 3132-3137.
(5) Kniazeva, T.; Hsiao, J. C.; Charest, J. L.; Borenstein, J. T. A Microfluidic Respiratory Assist Device with High Gas Permeance for Artificial Lung Applications. *Biomedical Microdevices* **2011,** *13* (2), 315-323.
(6) Fujii, T. PDMS-Based Microfluidic Devices for Biomedical Applications. *Microelectronic Engineering* **2002,** *61*, 907-914.
(7) Dittrich, P. S.; Manz, A. Lab-on-a-Chip: Microfluidics in Drug Discovery. *Nature Reviews Drug Discovery* **2006,** *5* (3), 210.
(8) Ertl, P.; Sticker, D.; Charwat, V.; Kasper, C.; Lepperdinger, G. Lab-on-a-Chip Technologies for Stem Cell Analysis. *Trends in Biotechnology* **2014,** *32* (5), 245-253.
(9) Selimović, Š.; Dokmeci, M. R.; Khademhosseini, A. Organs-on-a-Chip for Drug Discovery. *Current Opinion in Pharmacology* **2013,** *13* (5), 829-833.
(10) El-Ali, J.; Sorger, P. K.; Jensen, K. F. Cells on Chips. *Nature* **2006,** *442* (7101), 403.
(11) Wen, J. H.; Vincent, L. G.; Fuhrmann, A.; Choi, Y. S.; Hribar, K. C.; Taylor-Weiner, H.; Chen, S.; Engler, A. J. Interplay of Matrix Stiffness and Protein Tethering in Stem Cell Differentiation. *Nature Materials* **2014,** *13* (10), 979.
(12) Yim, E. K.; Darling, E. M.; Kulangara, K.; Guilak, F.; Leong, K. W. Nanotopography-Induced Changes in Focal Adhesions, Cytoskeletal Organization, and Mechanical Properties of Human Mesenchymal Stem Cells. *Biomaterials* **2010,** *31* (6), 1299-1306.
(13) Yim, E. K.; Pang, S. W.; Leong, K. W. Synthetic Nanostructures Inducing Differentiation of Human Mesenchymal Stem Cells into Neuronal Lineage. *Experimental Cell Research* **2007,** *313* (9), 1820-1829.
(14) Shao, Y.; Mann, J. M.; Chen, W.; Fu, J. Global Architecture of the F-Actin Cytoskeleton Regulates Cell Shape-Dependent Endothelial Mechanotransduction. *Integrative Biology* **2014,** *6* (3), 300-311.
(15) Serena, E.; Figallo, E.; Tandon, N.; Cannizzaro, C.; Gerecht, S.; Elvassore, N.; Vunjak-Novakovic, G. Electrical Stimulation of Human Embryonic Stem Cells: Cardiac Differentiation and the Generation of Reactive Oxygen Species. *Experimental Cell Research* **2009,** *315* (20), 3611-3619.
(16) Ehrbar, M.; Rizzi, S. C.; Hlushchuk, R.; Djonov, V.; Zisch, A. H.; Hubbell, J. A.; Weber, F. E.; Lutolf, M. P. Enzymatic Formation of Modular Cell-Instructive Fibrin Analogs for Tissue Engineering. *Biomaterials* **2007,** *28* (26), 3856-3866.
(17) Jansen, L.; McCarthy, T.; Lee, M.; Peyton, S. A synthetic, three-dimensional bone marrow hydrogel. *bioRxiv* **2018**, 275842.
(18) Tan, S. H.; Nguyen, N.-T.; Chua, Y. C.; Kang, T. G. Oxygen Plasma Treatment for Reducing Hydrophobicity of a Sealed Polydimethylsiloxane Microchannel. *Biomicrofluidics* **2010,** *4* (3), 032204.
(19) Olander, B.; Wirsén, A.; Albertsson, A.-C. Argon Microwave Plasma Treatment and Subsequent Hydrosilylation Grafting as a Way to Obtain Silicone Biomaterials with Well-Defined Surface Structures. *Biomacromolecules* **2002,** *3* (3), 505-510.
(20) Berdichevsky, Y.; Khandurina, J.; Guttman, A.; Lo, Y.-H. UV/Ozone Modification of Poly(Dimethylsiloxane) Microfluidic Channels. *Sensors and Actuators B: Chemical* **2004,** *97* (2-3), 402-408.
(21) Maji, D.; Lahiri, S.; Das, S. Study of Hydrophilicity and Stability of Chemically Modified PDMS Surface Using Piranha and KOH Solution. *Surface and Interface Analysis* **2012,** *44* (1), 62-69.
(22) Boxshall, K.; Wu, M. H.; Cui, Z.; Cui, Z.; Watts, J. F.; Baker, M. A. Simple Surface Treatments to Modify Protein Adsorption and Cell Attachment Properties within a Poly(Dimethylsiloxane) Micro-Bioreactor. *Surface and Interface Analysis* **2006,** *38* (4), 198-201.
(23) Kuddannaya, S.; Chuah, Y. J.; Lee, M. H. A.; Menon, N. V.; Kang, Y.; Zhang, Y. Surface Chemical Modification of Poly(Dimethylsiloxane) for the Enhanced Adhesion and Proliferation of Mesenchymal Stem Cells. *ACS Applied Materials & Interfaces* **2013,** *5* (19), 9777-9784.

(24) Li, B.; Chen, J.; Wang, J. H. C. RGD Peptide-Conjugated Poly(Dimethylsiloxane) Promotes Adhesion, Proliferation, and Collagen Secretion of Human Fibroblasts. *Journal of Biomedical Materials Research Part A* **2006,** *79* (4), 989-998.
(25) Chuah, Y. J.; Koh, Y. T.; Lim, K.; Menon, N. V.; Wu, Y.; Kang, Y. Simple Surface Engineering of Polydimethylsiloxane with Polydopamine for Stabilized Mesenchymal Stem Cell Adhesion and Multipotency. *Scientific Reports* **2015,** *5*, 18162.
(26) Yang, F. K.; Zhao, B. Adhesion Properties of Self-Polymerized Dopamine Thin Film. *Open Surf. Sci. J* **2011,** *3* (2), 115-122.
(27) Lee, H.; Scherer, N. F.; Messersmith, P. B. Single-Molecule Mechanics of Mussel Adhesion. *Proceedings of the National Academy of Sciences* **2006,** *103* (35), 12999-13003.
(28) Lee, H.; Dellatore, S. M.; Miller, W. M.; Messersmith, P. B. Mussel-Inspired Surface Chemistry for Multifunctional Coatings. *Science* **2007,** *318* (5849), 426-430.
(29) Wang, J. L.; Ren, K. F.; Chang, H.; Jia, F.; Li, B. C.; Ji, Y.; Ji, J. Direct Adhesion of Endothelial Cells to Bioinspired Poly(Dopamine) Coating Through Endogenous Fibronectin and Integrin α5β1. *Macromolecular Bioscience* **2013,** *13* (4), 483-493.
(30) Rübsam, K.; Stomps, B.; Böker, A.; Jakob, F.; Schwaneberg, U. Anchor Peptides: A Green and Versatile Method for Polypropylene Functionalization. *Polymer* **2017,** *116*, 124-132.
(31) Rübsam, K.; Davari, M. D.; Jakob, F.; Schwaneberg, U. KnowVolution of the Polymer-Binding Peptide LCI for Improved Polypropylene Binding. *Polymers* **2018,** *10* (4), 423.
(32) Schmidtchen, A.; Pasupuleti, M.; Malmsten, M. Effect of Hydrophobic Modifications in Antimicrobial Peptides. *Advances in Colloid and Interface Science* **2014,** *205*, 265-274.
(33) Noor, M.; Dworeck, T.; Schenk, A.; Shinde, P.; Fioroni, M.; Schwaneberg, U. Polymersome Surface Decoration by an EGFP Fusion Protein Employing Cecropin A as Peptide "Anchor". *Journal of Biotechnology* **2012,** *157* (1), 31-37.
(34) Rübsam, K.; Weber, L.; Jakob, F.; Schwaneberg, U. Directed Evolution of Polypropylene and Polystyrene Binding Peptides. *Biotechnology and Bioengineering* **2018,** *115* (2), 321-330.
(35) Gong, W.; Wang, J.; Chen, Z.; Xia, B.; Lu, G. Solution Structure of LCI, a Novel Antimicrobial Peptide from Bacillus Subtilis. *Biochemistry* **2011,** *50* (18), 3621-3627.
(36) Horinek, D.; Serr, A.; Geisler, M.; Pirzer, T.; Slotta, U.; Lud, S.; Garrido, J.; Scheibel, T.; Hugel, T.; Netz, R. Peptide Adsorption on a Hydrophobic Surface Results from an Interplay of Solvation, Surface, and Intrapeptide Forces. *Proceedings of the National Academy of Sciences* **2008,** *105* (8), 2842-2847.
(37) Dedisch, S.; Wiens, A.; Davari, M. D.; Söder, D.; Rodriguez-Emmenegger, C.; Jakob, F.; Schwaneberg, U. Matter-Tag: A Universal Immobilization Platform for Enzymes on Polymers, Metals, and Silicon-Based Materials. *Biotechnology and Bioengineering* **2019**.
(38) Grimm, A. R.; Sauer, D. F.; Mirzaei Garakani, T.; Rübsam, K.; Polen, T.; Davari, M. D.; Jakob, F.; Schiffels, J.; Okuda, J.; Schwaneberg, U. Anchor Peptide-Mediated Surface Immobilization of a Grubbs-Hoveyda-Type Catalyst for Ring-Opening Metathesis Polymerization. *Bioconjugate Chemistry* **2019,** *30* (3), 714-720.
(39) Zhou, Q.; Kühn, P. T.; Huisman, T.; Nieboer, E.; Van Zwol, C.; Van Kooten, T. G.; Van Rijn, P. Directional Nanotopographic Gradients: a High-Throughput Screening Platform for Cell Contact Guidance. *Scientific Reports* **2015,** *5*, 16240.
(40) Zhou, Q.; Castañeda Ocampo, O.; Guimarães, C. F.; Kühn, P. T.; van Kooten, T. G.; van Rijn, P. Screening Platform for Cell Contact Guidance Based on Inorganic Biomaterial Micro/Nanotopographical Gradients. *ACS Applied Materials & Interfaces* **2017,** *9* (37), 31433-31445.
(41) Rose, J. C.; Gehlen, D. B.; Haraszti, T.; Köhler, J.; Licht, C. J.; De Laporte, L. Biofunctionalized Aligned Microgels Provide 3D Cell Guidance to Mimic Complex Tissue Matrices. *Biomaterials* **2018,** *163*, 128-141.
(42) Arai, R.; Ueda, H.; Kitayama, A.; Kamiya, N.; Nagamune, T. Design of the Linkers which Effectively Separate Domains of a Bifunctional Fusion Protein. *Protein Engineering* **2001,** *14* (8), 529-532.
(43) Kapust, R. B.; Tözsér, J.; Fox, J. D.; Anderson, D. E.; Cherry, S.; Copeland, T. D.; Waugh, D. S. Tobacco Etch Virus Protease: Mechanism of Autolysis and Rational Design of Stable Mutants with Wild-Type Catalytic Proficiency. *Protein Engineering* **2001,** *14* (12), 993-1000.
(44) Laemmli, U. K. Cleavage of Structural Proteins During the Assembly of the Head of Bacteriophage T4. *Nature* **1970,** *227* (5259), 680.

(45) Blanusa, M.; Schenk, A.; Sadeghi, H.; Marienhagen, J.; Schwaneberg, U. Phosphorothioate-Based Ligase-Independent Gene Cloning (PLICing): An Enzyme-Free and Sequence-Independent Cloning Method. *Analytical Biochemistry* **2010,** *406* (2), 141-146.
(46) Bryksin, A. V.; Matsumura, I. Overlap Extension PCR Cloning: a Simple and Reliable Way to Create Recombinant Plasmids. *Biotechniques* **2010,** *48* (6), 463-465.

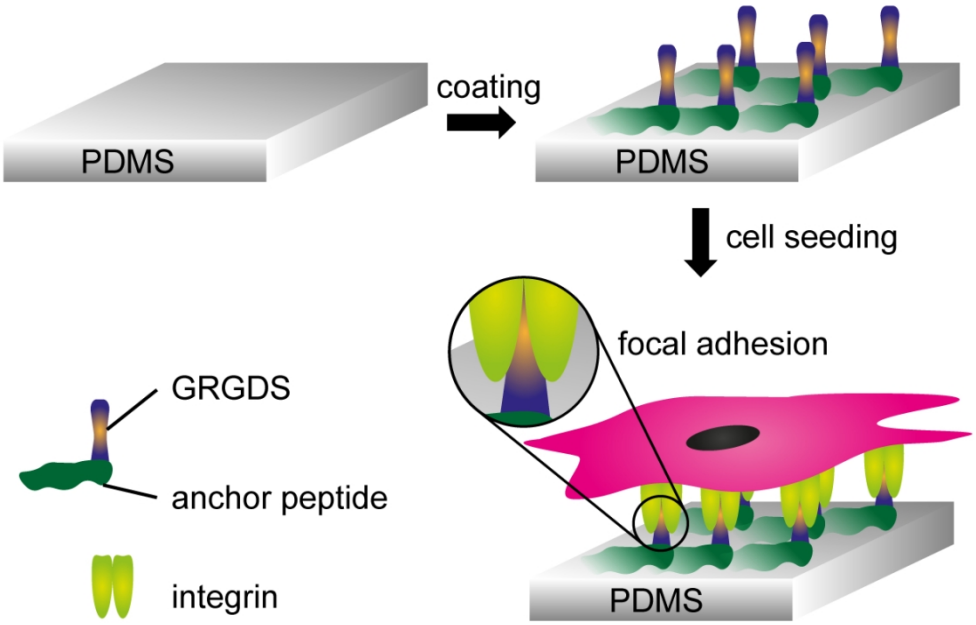

graphical abstract

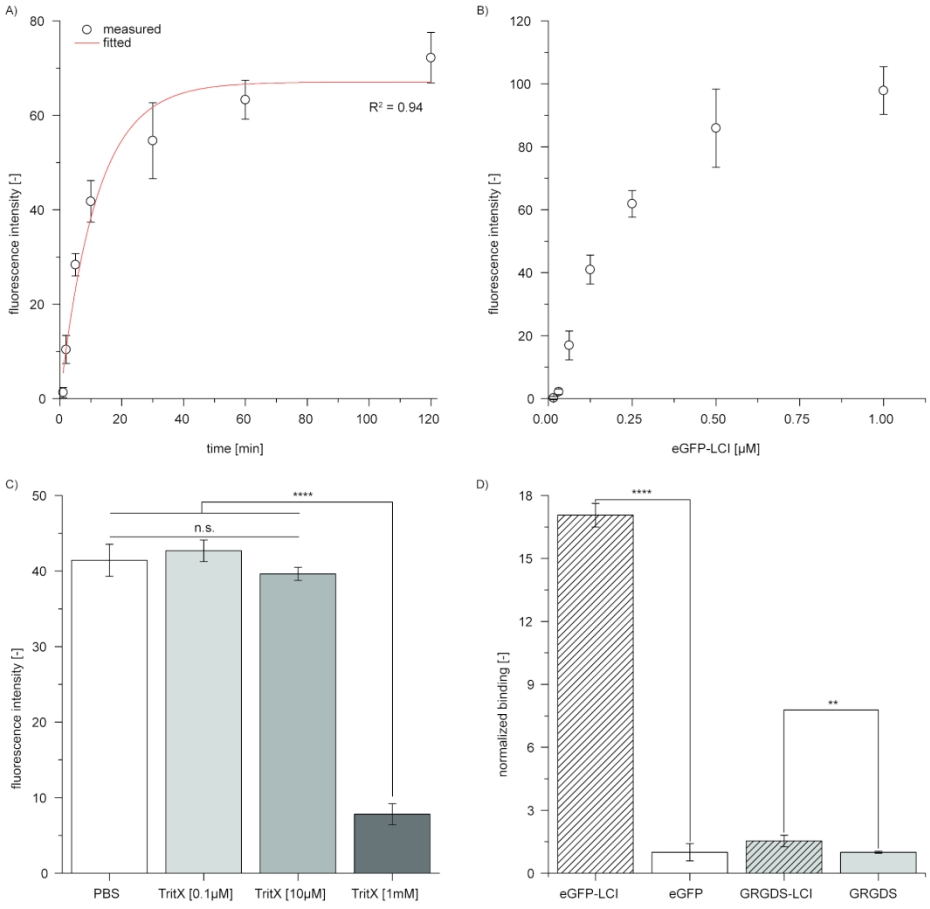
A)
measured
fitted
R² = 0.94
fluorescence intensity [-]
time [min]
B)
fluorescence intensity [-]
eGFP-LCI [µM]
C)
n.s.
****
fluorescence intensity [-]
PBS
TritX [0.1µM]
TritX [10µM]
TritX [1mM]
D)
****
**
normalized binding [-]
eGFP-LCI
eGFP
GRGDS-LCI
GRGDS

Figure 1

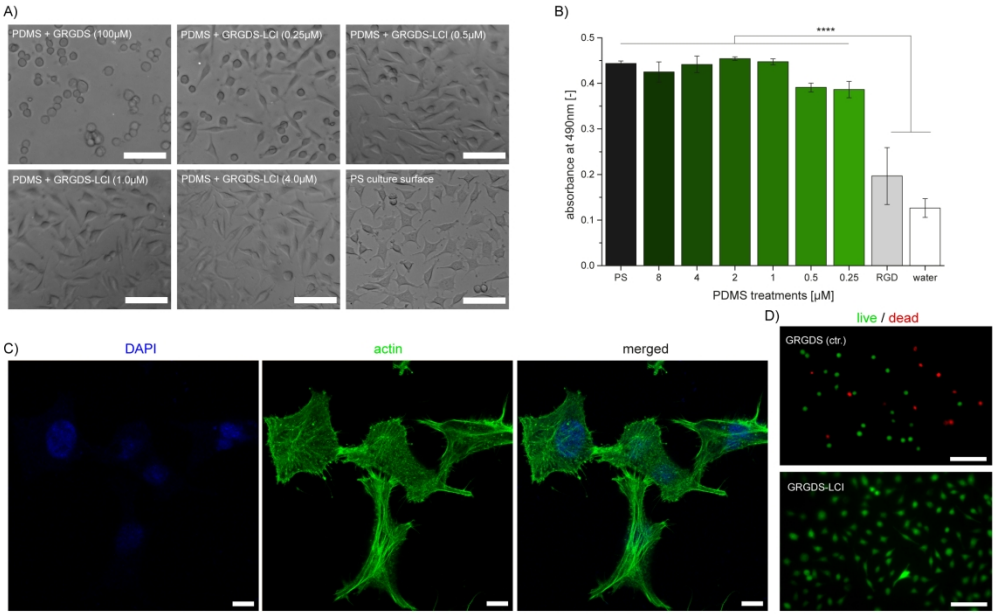
A)
PDMS + GRGDS (100µM)
PDMS + GRGDS-LCI (0.25µM)
PDMS + GRGDS-LCI (0.5µM)
PDMS + GRGDS-LCI (1.0µM)
PDMS + GRGDS-LCI (4.0µM)
PS culture surface
B)
****
absorbance at 490nm [-]
0.0
0.1
0.2
0.3
0.4
0.5
PS
8
4
2
1
0.5
0.25
RGD
water
PDMS treatments [µM]
C)
DAPI
actin
merged
D)
live / dead
GRGDS (ctr.)
GRGDS-LCI

Figure 2

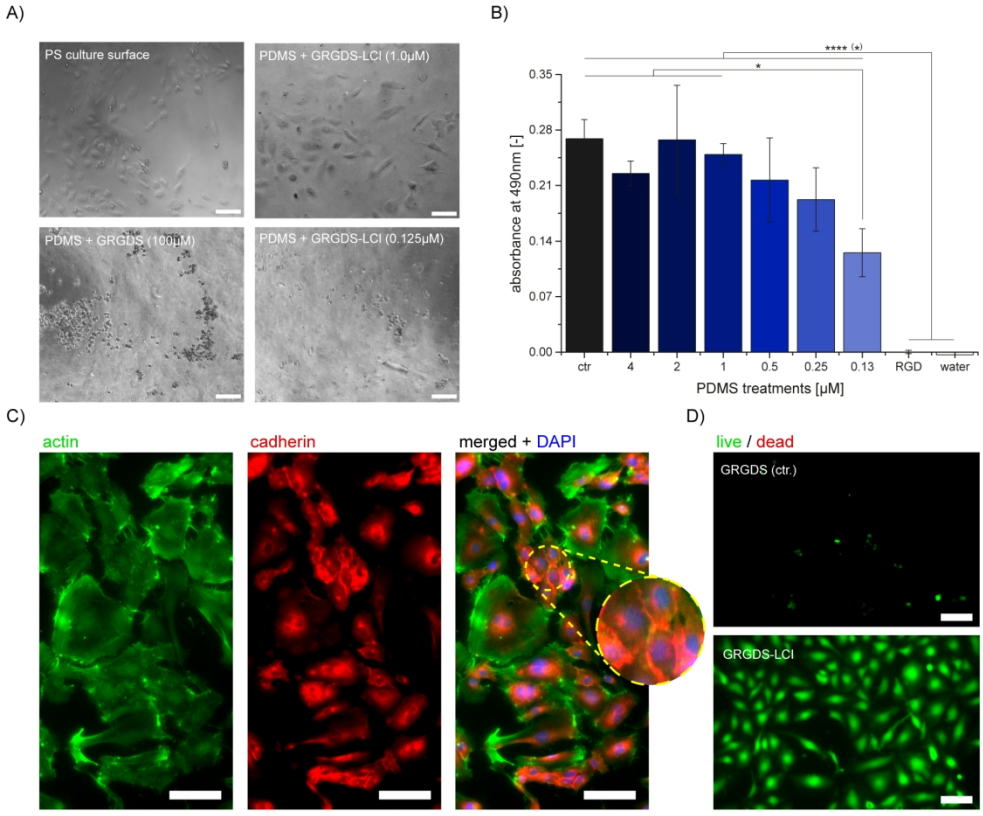
A)
PS culture surface
PDMS + GRGDS-LCI (1.0µM)
PDMS + GRGDS (100µM)
PDMS + GRGDS-LCI (0.125µM)
B)
absorbance at 490nm [-]
0.35
0.28
0.21
0.14
0.07
0.00
ctr
4
2
1
0.5
0.25
0.13
RGD
water
PDMS treatments [µM]
C)
actin
cadherin
merged + DAPI
D)
live / dead
GRGDS (ctr.)
GRGDS-LCI

Figure 3

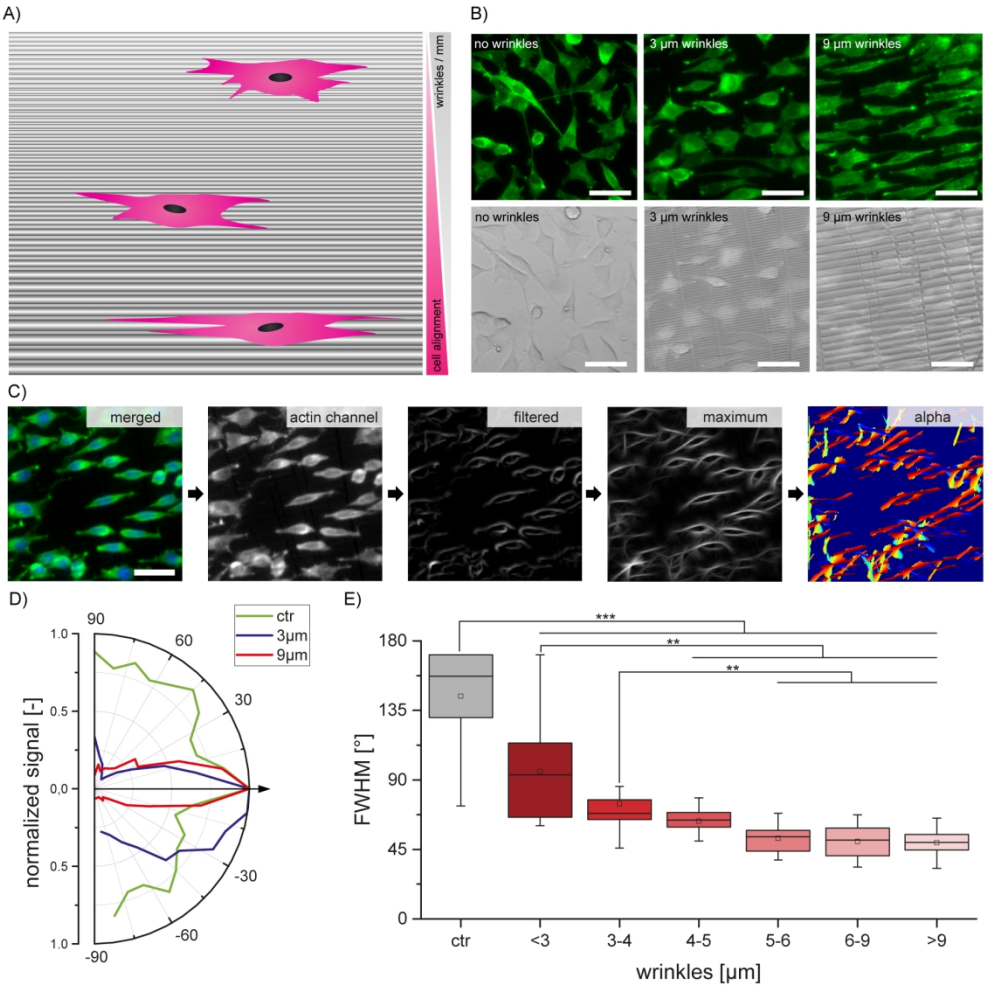
A)
wrinkles / mm
cell alignment
B)
no wrinkles
3 µm wrinkles
9 µm wrinkles
no wrinkles
3 µm wrinkles
9 µm wrinkles
C)
merged
actin channel
filtered
maximum
alpha
D)
ctr
3µm
9µm
normalized signal [-]
90
60
30
-30
-60
-90
1.0
0.5
0.0
0.5
1.0
E)
FWHM [°]
180
135
90
45
0
***
**
**
ctr
<3
3-4
4-5
5-6
6-9
>9
wrinkles [µm]

Figure 4